Hydraulic Properties of a Desert Soil Chronosequence in the Mojave Desert, USA

M. H. Young,* E. V. McDonald, T. G. Caldwell, S. G. Benner, and D. G. Meadows

ABSTRACT

Desert pavements are prominent features in arid environments and consist of a surface layer of closely packed gravel that overlies a thin, gravel-poor, vesicular A (Av) soil horizon. Well-developed Av horizons form distinct and highly structured columnar peds. These structures, along with their silt- and clay-rich texture, are hypothesized as controlling infiltration and hence the overall hydrologic conditions in the soil profile. The objectives of this study were to (i) evaluate how pedological development in near-surface soil horizons in an arid alluvial fan complex affects the soil hydraulic characteristics, and (ii) to compare the use of Wooding's equation and inverse modeling for evaluating hydraulic conductivity in highly layered, near-surface soils. These objectives were approached through field tension infiltrometer studies, soil sampling, and laboratory analyses of soil texture, water content, and soluble salt concentrations. Soils at five sites were studied at the Mojave National Preserve, California, representing a soil chronosequence (50–100 000 yr) with varying degrees of desert pavement development. Results indicated 100-fold and threefold declines, respectively, in saturated hydraulic conductivity (K_s) with both analytical methods, and α_w using Wooding's method, as the soils aged. No clear trends in K_s or α_w were detected in the underlying horizon, indicating that the controlling feature at these sites, in terms of water entry, was the K_s of the surface (Av) horizon. Soluble salt concentrations within the profile indicated reduced infiltration with increased pavement development. Results showed that surface age can be used as an excellent predictor of saturated hydraulic conductivity ($r^2 = 0.9254$). Further, results suggest that Av horizon development represents a key process controlling water cycling, potentially influencing ecosystem function in arid lands.

Sustainable ecosystems in arid and semiarid environments require detailed knowledge of the dynamic relationships among geomorphology, soil hydrology, surface characteristics, and plant cover. This is especially important given the limited occurrence of rainfall events that produce significant local recharge or surface runoff that could lead to recharge at other focus areas (microtopographic lows or ephemeral washes). It is also important that these dynamic relationships be investigated before development in undisturbed arid areas is undertaken. Timely availability of new data will be useful in future decision-making processes because development of these fragile lands is likely to occur with or without the results of scientific research.

Desert pavements consist of a surface layer of closely packed gravel that overlies a thin (3–10 cm), fine-grained, gravel-poor, vesicular A (Av) soil horizon.[1] Desert pavements are prominent features in arid environments and can be found on a variety of landforms of significantly diverse ages ranging from Holocene to Tertiary (Bull, 1991; Cooke et al., 1993). Pavements have been used in subdividing and correlating Quaternary alluvial fans for studying neotectonics and Quaternary climate change (McFadden et al., 1998; Bull, 1991; McDonald et al., 2003). Other research has shown that age is an important consideration in development of desert pavements, especially in areas downwind of source zones for aeolian deposited material (McDonald, 1994; McDonald et al., 1996; McFadden et al., 1998). Pavements tend to be more prevalent and more strongly developed on older surfaces where aerosolic clay- and silt-sized particles are deposited on the surface and are subsequently translocated downward into the soil profile. Increasing accumulation of aerosolic fines with time enhances the development of a highly structured Av horizon consisting of distinct columnar-shaped peds, ranging in diameter from about 3 to 8 cm, that part to platy peds, ranging in thickness from 0.2 to 1 cm. The formation of desert pavement and the Av horizon is extremely slow and can take from 4000 to 10 000 yr to become established.

Hydraulic properties of structured soils have been studied for some time, primarily in environments different from the arid Mojave Desert. Some studies have shown that pedological development of clayey soils can explain dynamic water flow through cracks and other macropores (Lin et al., 1998, 1999; Bouma and Wosten, 1979; Jarvis and Messing, 1995). Others have sought to understand the pore classes that contributed the majority of flow (e.g., Watson and Luxmoore, 1986), many of which were also in clayey soils. The study described here is unique with respect to the significantly drier climate where the soils developed, the general lack of swelling clays in these arid climates, the difference in the time needed to develop the structure, and the fragility of these surfaces. Their disruption can have a potentially dramatic impact on water balance.

The understanding of how soil hydrology affects soil development spans a number of practical environmental applications. Knowledge of soil dynamics and the consequent linkages to ecosystem development will facilitate improved designs of evapotranspiration disposal covers, ultimately leading to stable and maintenance-free features on the landscape (Shafer et al., 2004). Soil hydrology plays an extremely important role in near-surface water balances and the associated responses in water-limited ecosystems. McDonald et al. (1996) demon-

M.H. Young, S.G. Benner, and D.G. Meadows, Desert Research Institute, Univ. and Community College System of Nevada, Las Vegas, NV 89119; E.V. McDonald and T.G. Caldwell, Desert Research Institute, Univ. and Community College System of Nevada, Reno, NV 89512; D.G. Meadows, currently, Hydrologic Sciences Program, Univ. of Nevada, Reno, NV 89532; S.G. Benner, currently, Dep. of Geosciences, Boise State Univ., Boise, ID 83725. Received 2 Nov. 2003. Original Research Paper. *Corresponding author (michael.young@dri.edu).

Published in Vadose Zone Journal 3:956–963 (2004).

677 S. Segoe Rd., Madison, WI 53711 USA

[1] The lower case letter v formally stands for the presence of plinthite (Soil Survey Staff, 1998); however the v has been extensively used in a substantial number of studies of desert soils that possess horizons with abundant vesicular pores.

strated that the interrelated control of soil development and climate variation on soil water flux explains temporal variations in the depth of soil carbonates. Hammerlynck et al. (2002) used soil water potential data and desert shrub responses in Mojave Desert soils of different age and parent material to show that plant responses were strongly affected by soil age. These two studies (conducted at the same sites used in the present study) concluded that the depth of water infiltration was partly responsible for soil and ecosystem effects; however, these studies did not comprehensively quantify the hydraulic properties of the Av horizon. Briones et al. (1998) showed how interspecies competition increased when supplemental irrigation was used on study plots in the Chihuahuan Desert and how available soil water was partitioned among existing dominant species, with no interspecies competition. Porporato et al. (2002) developed a probabilistic framework showing how statistical distributions of soil hydraulic conductivity can be used as a tool for estimating ecosystem responses to different soil water balances. These results provide insight into ecosystem evolution in desert environments and the strong linkage between soil development, water cycling, desert ecosystem function, and desert landscape management and restoration.

Ecosystems are highly dependent on soil recharge in water-limited desert environments (Eagleson, 2002). However, detailed knowledge of the hydrological behaviors of different soils and geomorphic settings is needed to advance our understanding of many ecological processes, ranging from local to landscape-level ecosystems. We are aware of limited investigations on infiltration into soils of variable pavement development (Brown and Dunkerley, 1996; McDonald, 1994; McDonald et al., 1996), and these studies primarily focused on measuring infiltration capacity. The research reported herein extends the work of McDonald (1994) and seeks to provide a strong foundation to better understand the role of pavements in the hydrologic cycle of arid environments. We quantify, for the first time, how hydraulic properties covary with time in arid environments where desert pavements form.

The objectives of this work are to (i) evaluate how pedological development in near-surface soil horizons in an arid alluvial fan complex can affect soil hydraulic characteristics and (ii) to compare the use of Wooding's equation and inverse modeling for evaluating hydraulic conductivity in highly layered soils. These objectives were approached through field tension infiltrometer studies, soil sampling, and laboratory analyses of soil texture, water content, and soluble salt concentrations.

MATERIALS AND METHODS

Field measurements were taken within the Mojave National Preserve (bounded between 115.61 and 115.39°N latitude and 35.31 and 34.83°N longitude), approximately 150 km south-southwest of Las Vegas, NV. The preserve is located on a broad alluvial fan complex consisting of four different parent materials: limestone, mixed plutonics, quartz monzonite, and mixed volcanics. Precipitation and vegetation vary widely depending on elevation. Precipitation averages between 130 and 230 mm yr^{-1} where the tests were conducted, with at least 25% falling in localized summer monsoon thunderstorms. Common plants include creosote bush [*Larrea tridentata* (Sessé & Moc. ex DC.) Coville], white bursage [*Ambrosia dumosa* (A. Gray) W.W. Payne], and yucca (*Yucca* spp.). Plant size and vegetative cover vary widely depending on the pedological development of surface soil and the presence or absence of petrocalcic and argillic horizons.

The tests described here were constrained on soils composed of mixed plutonic parent material. General descriptions are presented in Table 1. Detailed descriptions and interpretation of soils measured in this investigation are provided in McDonald (1994) and McDonald et al. (1996, 2003). The sites chosen for measurement and analyses differed primarily in age, thus constituting a chronosequence from recent to approximately 100 000 yr old (100 ka). Soil surfaces were classified according to the nomenclature QfX, where Q represents Quaternary Period, f represents fluvial or fan, and X represents the subclassification that ranges from 8 to 1, denoting relative age (8 is most recent and 1 is oldest). For this research, soil surfaces of Qf8, Qf7, Qf6, Qf5, and Qf3 were used. These designations correspond to soil surfaces with ages of 0.05, 0.50, 4, 10, and 100 ka, respectively, as determined by McDonald et al. (2003) using local radiometric dates and soil-stratigraphic correlations to date deposits in nearby areas. Figure 1 is a conceptual diagram showing how the soil surface evolves with time both structurally and texturally. The increase in the thickness and structural integrity of the Av horizon is an aggradational process, where fines are transported by wind from upwind sources and then deposited. Over many millennia, the aeolian processes build up the fines content (silt plus clay) while the clasts slowly move upward (McFadden et al., 1987, 1998).

At each site, triplicate tension infiltrometer locations were identified for both the uppermost A horizon (pavement surfaces in most cases) and the underlying B horizon. Site treatment for the A horizon was limited to gently removing the surface clasts, which exposed the soil surface directly underneath and facilitated contact between the infiltrometer and soil (removing clasts made the measurements possible and focused results on our goal to study the vesiculated horizons). Small plants or other materials that could puncture the infiltrometer membrane were removed. Moistened contact sand was then placed on the soil surface. Sites used for the B horizon required excavation of 0 to 10 cm of overlying material depending on age. Locating the bottom of the surface (Av) horizon was straightforward in most cases because the peds

Table 1. Descriptions of soils used in this study. Data taken from McDonald (1994).

Qf8	Qf7	Qf6	Qf5	Qf3
		Soil classification		
Typic Torriorthents	Typic Torriorthents	Typic Haplocambids	Typic Haplocambids	Calcic Paleargids
	Horizon designations, depths (cm), bulk densities (g cm^{-3})			
	A, 0–2, 1.8	Av, 0–3, 1.75	Av, 0–4, 1.69	Av, 0–6, 1.71
	AC, 2–9 cm, 1.8	Abv, 3–27, 1.95	Bwk, 4–12, 1.73	Bt, 6–26, 1.71
C, 0–50+, 1.70	Ck1, 9–50+, 2.34	Ck1, 27–50+, 2.13	Btk, 12–50+, 2.02	Btk, 26–50+, 1.84

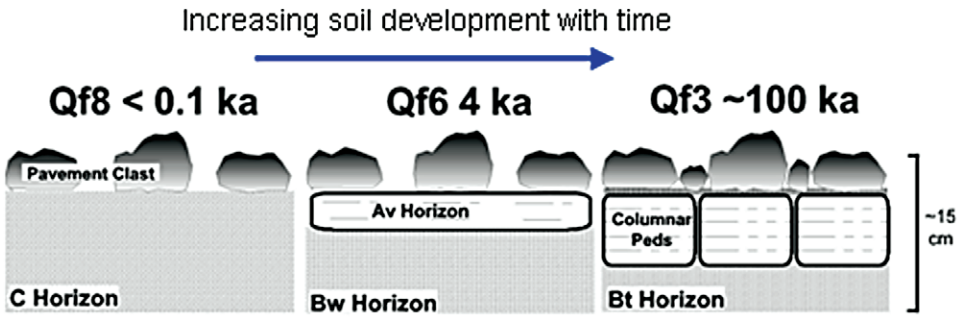

Fig. 1. Conceptual diagram showing how the soil surfaces age with time. Qf indicates Quaternary fluvial deposits, ka indicates thousands of years old, Av indicates vesicular A horizon, Bw indicates a B horizon with some color or structural development, Bt indicates a B horizon with clay accumulation, and C horizon indicates material that has little pedogenic development. Note that Av horizon was not present on the younger surfaces (Qf7, Qf8).

remained intact when removed and because of a noticeable increase in soil rubification within the B horizon. Before conducting the infiltration test, we collected grab samples, which were analyzed for initial water content.

Data from the infiltrometers (Soil Measurement Systems, Tucson, AZ) were collected from differential pressure transducers (Casey and Derby, 2002) at intervals between 15 s and 1 min, depending on the logger unit and soil surface. Manual readings were taken periodically to verify operation and to better identify when the intake rate was at or near steady state. At that time, the infiltrometer was reset to a higher (less negative) pressure level. Four to five pressure steps were used for each test, typically at levels set to approximately −1.2, −0.9, −0.6, −0.3, and 0 (saturation) kPa.

At the conclusion of each test, the infiltrometer and contact sand were removed and another sample was taken for bulk density and final water content. Samples were taken with a soil ring (5-cm diameter, 2.5-cm height) pressed into the soil near the center of the infiltrated area. The ring was removed using a hand trowel and leveled appropriately to better define the sample volume. A soil pit was also excavated immediately adjacent to the infiltrometer test locations. Samples were collected at 5- to 10-cm interval depths throughout the upper 50 cm of the profile. Samples were stored in sealable, plastic bags to prevent water loss and were returned to the laboratory for further analyses. Particle-size distribution was determined using a Laser Light Scattering technique (model Saturn DigiSizer 5200, Micromeritics Instruments, Norcross, GA). Bulk density was determined using the clod method of Blake and Hartge (1986). Soluble salt (Ca, Mg, K, Na, and SO_4 as S) content was determined for samples from the soil pit profiles. One gram of dried soil was placed into a plastic bottle with 25 mL of distilled water and agitated for 24 h on an orbital shaker at 100 rpm. The liquid was then decanted, filtered (0.45 μm), and acidified to pH <2 using trace-grade HCl, before analyzing with an inductively coupled plasma spectrometer (Thermo Intrepid Radial ICP-EOS, Franklin, MA).

Data Analysis

Data were analyzed using a manual, semiempirical method (Wooding, 1968) and a numerical inverse method (Šimunek et al., 1999). The different methods were used to evaluate whether better estimates of hydraulic conductivity would be worth the extra postprocessing efforts required in the numerical method and because inverse modeling provides estimates of soil water retention properties, while Wooding's analysis does not. Wooding's analysis relies mostly on the data collected toward the end of each pressure step when the cumulative flux rate is constant in time and provides estimates of the saturated hydraulic conductivity and conductivity–water potential function, $K(h)$. Inverse modeling uses all the data and results in estimates of the conductivity and water content–water potential functions, $\theta(h)$.

Vertical infiltration is initially governed by capillarity or sorptivity of water into the soil matrix, containing both vertical and horizontal components. Later-time infiltration becomes gravity driven and linear with time as soil capillarity forces are reduced, indicating that infiltration is at steady state. Based on Gardner's exponential $K(h)$ function (Gardner, 1958), a three-dimensional, analytical solution for steady-state infiltration from a circular source was derived by Wooding (1968):

$$q(h) = K_{sw} \exp(\alpha_w h) \left(1 + \frac{4}{\pi r \alpha_w}\right) \qquad [1]$$

where $q(h)$ is the steady-state infiltration (cm s^{-1}), h is the soil water potential (expressed here in cm H_2O), K_{sw} is the saturated hydraulic conductivity (cm s^{-1}) obtained with Wooding's analysis, α_w is a parameter (cm^{-1}) affected by the pore-size distribution, and r is the infiltrometer radius (cm). The first term inside the bracket represents vertical gravity flow and the second term inside the bracket accounts for lateral movement due to capillarity. The resulting equation contains two unknowns, K_{sw} and α_w. Using the infiltrometer through a range of pressures, paired values of flux $\{q(h)\}$ and pressures (h) are obtained. These known values are input for a nonlinear least-squares regression routine to solve for the two unknowns by minimizing error through iterative solutions (Logsdon and Jaynes, 1993).

In addition to using Wooding's solution for obtaining K_{sw} and α_w, a complete set of hydraulic properties was obtained through numerical inversion of the cumulative infiltration data (mL s^{-1}) and the final water content. Inverse modeling was done with the HYDRUS-2D program (Šimunek et al., 1999). HYDRUS-2D is an axisymmetric finite element code that iteratively optimizes parameters found in the van Genuchten (1980) form of the soil water retention curve, and in the hydraulic conductivity equation derived by Mualem (1976) as modified by van Genuchten (1980). The retention curve has the form

$$\theta_e(h) = \frac{\theta(h) - \theta_r}{\theta_s - \theta_r} = \frac{1}{(1 + |\alpha_{vg} h|^n)^m} \quad h < 0 \qquad [2]$$

and the unsaturated hydraulic conductivity function is defined as

$$K(\theta) = K_{svg} \theta_e^{1/2} [1 - (1 - \theta_e^{1/m})^m]^2 \qquad [3]$$

where θ_e is the effective volumetric water content, θ_s is the saturated volumetric water content, θ_r is the residual water content, n and m are empirical parameters where the expres-

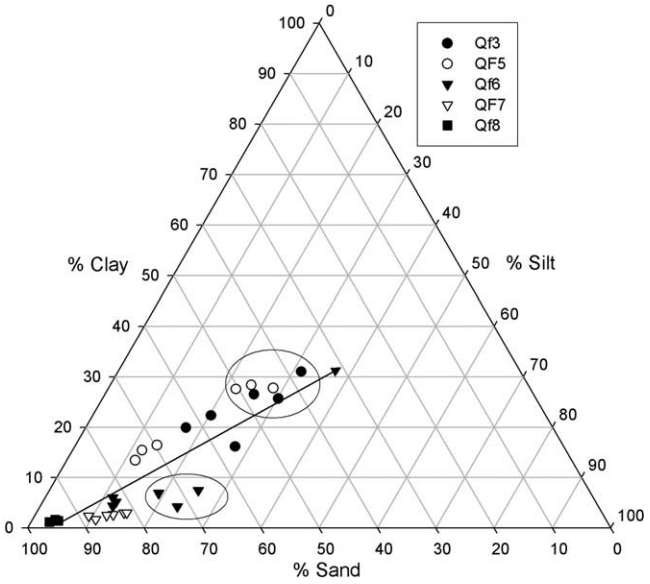

Fig. 2. Ternary diagram showing evolution of soil texture with time. Data points contained in circles refer to samples taken from the Av horizon, when that feature was present. Arrow points in direction of increasing soil age.

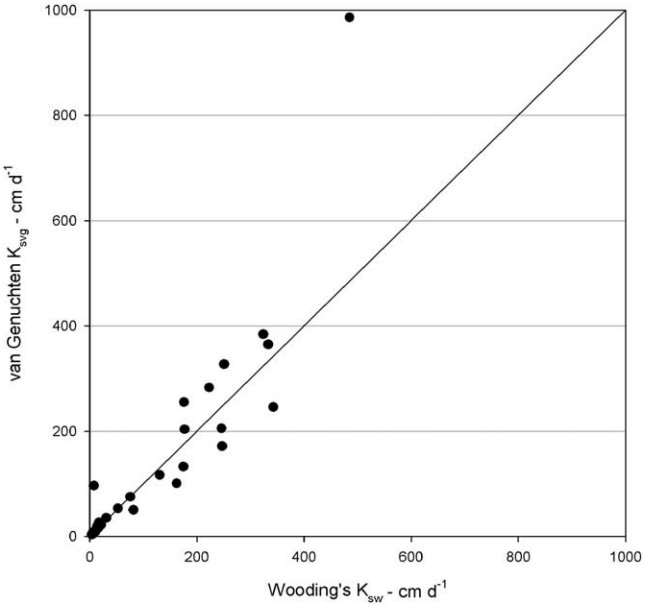

Fig. 3. Comparison between Wooding's K_{sw} vs. van Genuchten's K_{svg}, which was determined by inverse modeling. Symbols are data, and the line is the 1:1 line.

sion $m = 1 - 1/n$, α_{vg} (cm^{-1}) is an empirical fitting parameter similar, though not equal, to the inverse air entry value, and K_{svg} is the saturated hydraulic conductivity (cm s^{-1}).

The conceptual model consisted of a single-layered system for the younger soils and a multilayered system for older soils where the Av horizon had developed or was clearly present. In the former case, only one optimization was done to characterize the soil. In the latter case, two simulations were done. The first simulation optimized the parameters of the subsurface (B) horizon only, using data from that experiment. The second simulation fixed the parameters for the B horizon in a layered simulation where parameters for the surface (Av) horizon were optimized. This reduced the number of parameters to be optimized in any single simulation, thus increasing the potential for a unique set of parameters for each layer. This approach was similar to that suggested by Šimunek et al. (1998).

All conductivity data were normalized to 20°C. The correction factor was derived from known variation of water viscosity and density with temperature (Lide, 2001). An exponential relationship was obtained using TableCurve (Version 1.12, Jandel Scientific, San Rafeal, CA), and all saturated hydraulic conductivity data were adjusted accordingly. The correction factor, C, was

$$C = 0.2513 + 1.4983\exp(-T/28.8274) \quad [4]$$

where T was the temperature (°C) of the soil material following the field experiment. Furthermore, K_{sw} and K_{svg} were log-transformed before averaging to account for the lognormal distributions that they are known to exhibit (White and Sully, 1992; Mohanty and Mousli, 2000). The results of the data analyses were cross-correlated to evaluate the strength of association between age, physical properties, and hydraulic properties. Correlation tables were constructed to better identify and explain the most sensitive parameters affecting the hydraulic properties at these sites.

RESULTS AND DISCUSSION

Soil texture results are shown in Fig. 2, and they show an increase in fines (silt plus clay) content with increasing soil age and degree of development. The diagram shows the results for samples collected from the surface (Av) horizon and the underlying AC (Qf7) or B horizon (Qf6, Qf5, Qf3). Only the surface horizon was sampled from the Qf8 site because no distinct layering was present. The symbols on the diagram contained in the ellipses show that the fines content of the Av horizon is considerably greater relative to the fines content of the underlying AC or B horizons. The observed trend of increasing silt and clay content in the Av horizon with increasing soil age, relative to underlying soil horizons, is consistent with the results of soil texture analysis shown by McDonald (1994). Soil textures ranged from sand in Qf8 to clay loam in Qf5 and Qf3 soils.

Using coefficient of determination (r^2) as one measure of analytical success for the infiltrometer measurements, the minimum values obtained from the analyses were $r^2 = 0.816$ ($n = 4$) and $r^2 = 0.993$ ($n = 695$) using Wooding's analysis and inverse modeling, respectively. Both the analytical and numerical techniques closely reproduced field data. Only two tests using Wooding's analysis were found to have r^2 values <0.900, and each case was for the Qf3 soil, the most difficult to measure using the infiltrometer because of the very slow flow rate.

Figure 3 is a comparison of the two approaches, and the graph shows that both methods produced very similar conductivities. One outlier was identified using inverse modeling, but overall the data very closely grouped around the 1:1 line; $r^2 = 0.861$ ($n = 26$) without the outlier and $r^2 = 0.784$ ($n = 27$) with the outlier included. An analysis of variance of the two data sets indicated no reason to suspect that the data were sampled from different populations ($F = 0.2126$, $\alpha = 0.05$). No improvement in model results was found when sites with an Av surface horizon were represented as a two-

layered system. This finding is supported by the post sampling, which showed that wetting fronts did not penetrate beyond the Av horizon in older soils. Soil development apparently led to a higher water holding capacity. Therefore, the single-soil modeling approach for young soils was valid because no significant soil horizonation had developed, and it was valid for older soils because the wetting front remained within a single layer, the Av horizon. The results indicate that Wooding's analysis provided excellent estimates of hydraulic conductivity functions in this environment, but if estimates of water retention curves are needed, then inverse modeling is required.

Considering the finding that both the Wooding and inverse modeling approaches lead to similar estimates of saturated hydraulic conductivity for these materials, either approach can be used to show that saturated hydraulic conductivity of the surface soil is strongly age-dependent. Figure 4A shows a strong trend toward declining Wooding's K_{sw} values in the surface (Av) soil, especially between Qf7 and Qf6 surfaces (or between 0.5 and 4 ka, respectively) when a nearly 10-fold decline was measured. A pronounced decrease in infiltration between the Qf7 and Qf6 surfaces is consistent with the results of McDonald et al. (1996). In contrast, no trend or otherwise decline was observed in the subsurface (B) horizon. Although some increases in fines (with increasing age) were recorded in underlying soil layers, little associated change in soil structure was observed, likely explaining the relative insensitivity of conductivity with age. The α_w parameter, used in Eq. [1], also shows a clear decrease with increasing age in the surface horizon (Fig. 4B); again, no trend was observed in the subsurface horizon. Higher values of α_w lead to faster declines in unsaturated hydraulic conductivity with decreasing soil water potential (or decreasing water content). Thus, the approximately threefold reduction of α_w from 0.297 to 0.085 cm^{-1} from Qf8 to Qf3, respectively, will lead to substantially different $K(h)$ functions and potential for fluid-dominated flow. For example, if unsaturated hydraulic conductivity is calculated for the observed range of α_w and for uniform K_{sw} of 100 cm d^{-1}, the difference of hydraulic conductivity at a soil water potential equal to −10 kPa would exceed nine orders of magnitude, from 1.29×10^{-11} to 0.019 cm d^{-1}. Fluid flow at 10^{-11} cm d^{-1} would be considered very low to negligible in many practical applications. These results highlight the importance of quantifying the dependence of $K(h)$ on soil water potential (or soil water content) in predicting hydraulic behavior of these soils.

Table 2 shows the correlation matrix that compares the soil physical properties to the log-averaged hydraulic properties using the Wooding and inverse modeling approaches. The results are presented for the analyses of the surface horizon only because it is primarily the surface horizon that exhibited changes in soil hydraulic properties. Log-transformed soil age and hydraulic conductivity were added to be consistent with Fig. 4 and 5. The data show a very strong correlation between surface age and textural components. Aging corresponds to a reduction in sand content and an increase in silt and clay

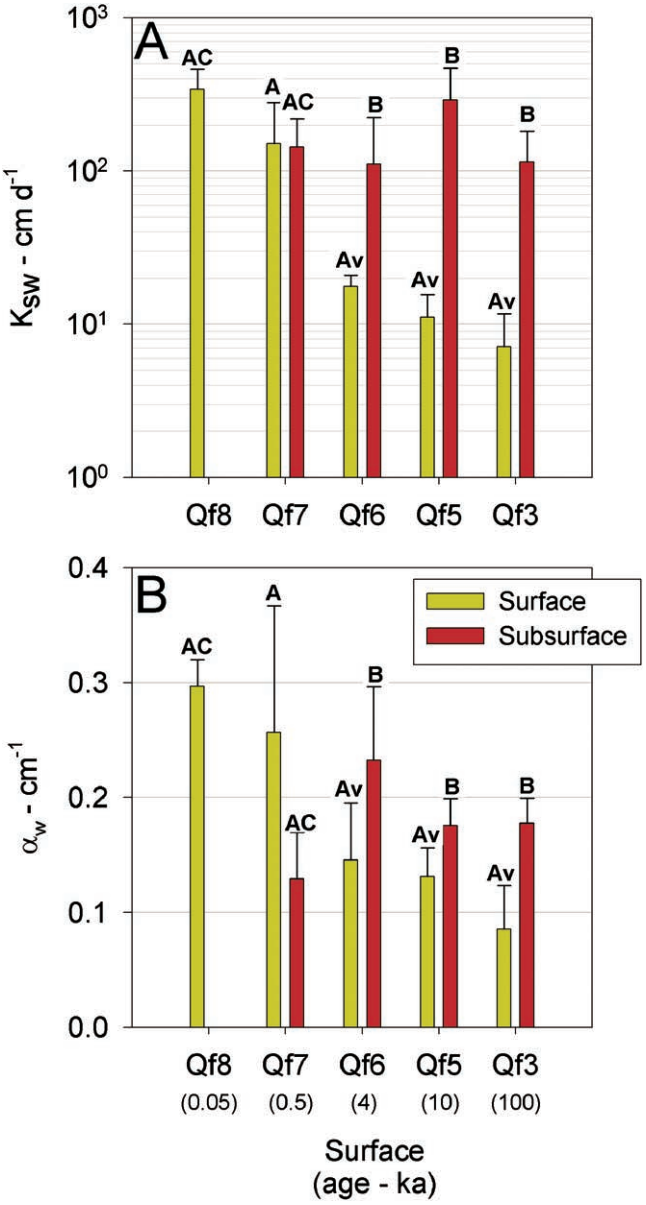

Fig. 4. Results of analysis for (A) K_{sw} and (B) α_w for different surface designations (*x* axis label) and soil layers (letter designations above error bars). Error bars represent standard deviations.

contents. The correlations of log age vs. the averages of the log hydraulic conductivity for both the Wooding (K_{sw}) and inverse modeling analyses (K_{svg}) were also found to have high statistical significance ($p = 0.001$ level). Also notable is the strong positive correlation between α_w and the sand percentage ($r = 0.80$, $n = 15$), which reflects the faster reduction in conductivity due to enhanced soil drainability. Correlation between α_{vg} and the soil textural components also fits the conceptual model that younger soils have more sand, higher drainability, and higher hydraulic conductivity. Overall, the conceptual model of hydraulic behavior in variably saturated soil was represented well in these analyses.

Predicting conductivity functions from surface age could have many benefits, from rapid assessments of surface runoff potential to predictions of landscape scale

Table 2. Correlation coefficients among age, physical properties, and hydraulic properties of the Av surface-soil horizon.†

	Age	log age	Bulk density	Gravel %	Sand %	Total silt %	<4 um %	K_{sw}	log K_{sw}	α_w	α_{vg}	n	K_{svg}	log K_{svg}
Age	1													
log age	0.76	1												
Bulk density	0.06	0.01	1											
Gravel %	−0.16	−0.55*	0.61*	1										
Sand %	−0.64*	−0.93***	0.31	0.76**	1									
Total silt %	0.63*	0.96***	−0.07	−0.62*	−0.93***	1								
<4 um %	0.58*	0.80***	−0.47	−0.79***	−0.96***	0.78***	1							
K_{sw}	−0.41	−0.83***	0.03	0.51	0.79***	−0.89***	−0.63*	1						
log K_{sw}	−0.59*	−0.93***	−0.01	0.51	0.90***	−0.95***	−0.77***	0.92***	1					
α_w	−0.58*	−0.84***	−0.05	0.41	0.80***	−0.84***	−0.69**	0.89***	0.93***	1				
α_{vg}	−0.48	−0.68**	−0.05	0.25	0.59*	−0.66**	−0.47	0.81***	0.71**	0.85***	1			
n	−0.31	−0.43	0.20	0.59*	0.48	−0.42	−0.48	0.11	0.30	0.14	−0.05	1		
K_{svg}	−0.33	−0.68**	0.07	0.38	0.62*	−0.72**	−0.47	0.93***	0.75**	0.75**	0.82***	−0.06	1	
log K_{svg}	−0.60*	−0.87***	−0.11	0.32	0.77***	−0.85***	−0.63*	0.90***	0.91***	0.92***	0.89***	0.07	0.82***	1

*** Significant at the 0.05 probability level.**
**** Significant at the 0.01 probability level.**
***** Significant at the 0.001 probability level.**
† All correlations based on 15 paired observations; all correlation coefficients reduced to two significant digits for display.

water contents. Thus, it is important that more than 90% of the variation in log K_{sw} could be attributed to the log soil age (Fig. 5). This relation illustrates that, even with the significant heterogeneity in soil-forming processes and the complexity of alluvial fan hydrology, many independent variables can be adequately accounted for by a single parameter, namely surface age. We hypothesize that the slope of this regression line will differ depending on parent material (especially the presence of feldspar minerals that weather into clays) and landscape position relative to aeolian source areas. However, surface age is not known at most locations, which makes evaluation of this hypothesis difficult. Furthermore, this trend is consistent with the recent work of Shafer et al. (2004), who showed similar trends in progressively older soil surfaces with parent materials that differed from this study.

This work demonstrates that pedogenic development leads to large differences in hydraulic properties of the surface soil. These differences will affect infiltration rates during precipitation events, and subsequently, the depth of percolation and evaporative losses. To evaluate deep percolation potential for these five profiles, water-soluble salt concentrations were determined for Ca, Mg, K, Na, and SO_4 as S. Profiles for Na are shown in Fig. 6A (profiles for all of these ions exhibited similar trends). Sodium concentrations were low (<100 g m^{-3}) across the entire profile for Qf8, Qf7, and Qf6, indicating that percolating waters have removed these salts from the profile. In contrast, the profiles from areas of well-developed pavements (Qf5 and Qf3) exhibited elevated Na concentrations. At the base of Qf5 profile, soluble Na concentrations reached 500 g m^{-3}, suggesting the maximum depth of percolation approached the bottom of the profile. On the Qf3 profile, peak values of >2500 g m^{-3} were observed at a depth of approximately 22.5 cm.

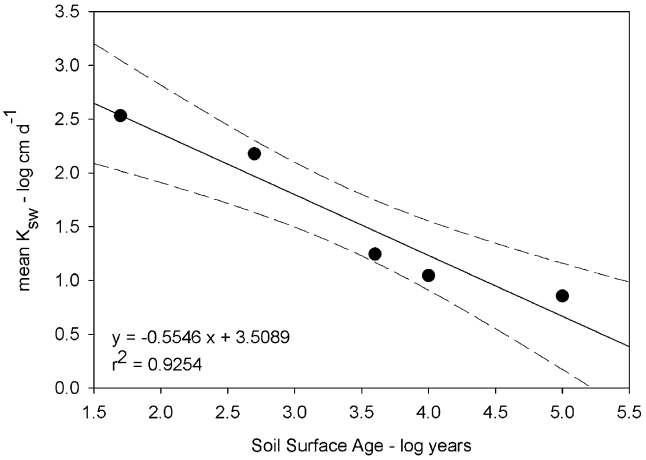

Fig. 5. Plot showing the relationship between soil surface age and mean K_{sw} for soils ranging in designation from Qf8 (young) to Qf3 (old). Solid line is linear regression, and dashed line is predictive error (95% confidence).

The measured decrease in hydraulic conductivity observed with desert pavement development and the marked decline in the depth of percolation are manifested in the soluble salt profiles underlying the surfaces investigated. These results are consistent with the work of Phillips (1994), who showed that soluble salt profiles in desert soils are characterized by low concentrations near the soil surface, a peak in concentration a few meters below ground surface, and decreasing concentrations below that depth. Therefore, salt content profiles can provide an indication of longer-term behavior of water infiltration and subsequent deep percolation. The depth of the salt peak can be closely correlated to the amount of water that enters the profile: higher amounts of infiltration result in a deeper salt peak.

Figure 6B shows water content profiles 4 d after a slow-moving frontal storm left 3.9 cm of precipitation. The water content profiles suggest that differences in the water holding capacity are also strongly influenced by pedological development. For example, the observed trend of lower water contents with decreasing age (i.e., Qf8–Qf6) can be attributed to higher downward drainage and/or upward evapotranspiration. These results suggest that the water holding capacity in near-surface soils increased with increasing soil age and degree of soil development. The clearly increasing progression of near-surface water content and the total soil water storage within that profile (Fig. 7) correspond well with the increasing fines content shown in Fig. 2 and Table 1.

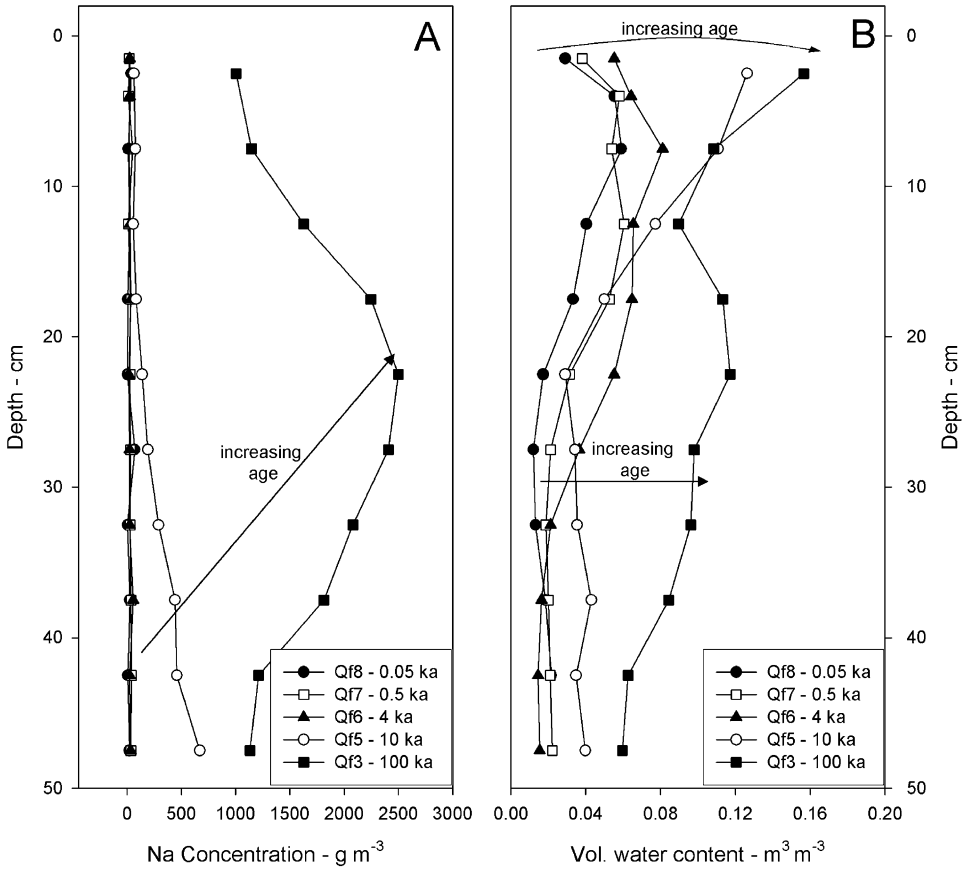

Fig. 6. (A) Sodium and (B) water content profiles for soils of different ages, taken 4 d after a 3.9-cm precipitation event. Soil ages are included in the legend for clarity.

CONCLUSIONS

Although this study is not complete in terms of representing all soil types or environments, the results show the importance of time on soil development and a significant effect on the hydraulic conductivity. The time period for soil surfaces to evolve from massive to blocky structure due to aeolian deposition and eventual translocation of silt and clay deeper into profile can take thousands of years depending on the proximity to source areas for fines and other environmental factors that control soil formation. The speed with which soils develop in arid climates and the resulting control on soil hydrology have several implications that need to be considered when evaluating land development or rehabilitation, landfill cover design, and overall ecosystem health in studies of climate change (McDonald, 2002).

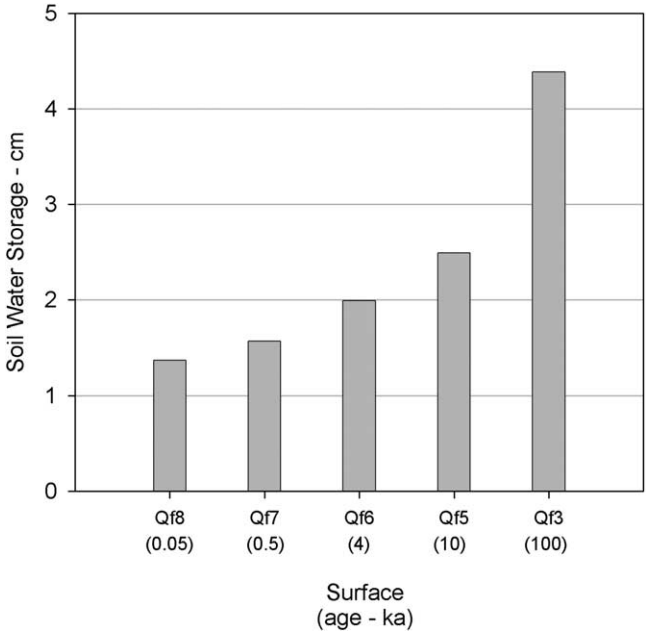

Fig. 7. Soil water storage measured in upper 50 cm of soil profile 4 d following a 3.9-cm precipitation event.

Pedological development of these surfaces impacts the water cycle in two important ways. First, lower hydraulic conductivities of this chronosequence dramatically limit infiltration and, by inference, will likely increase runoff. This will reduce the amount of water that percolates to plant roots and potentially increase the flux of water to ephemeral washes. Second, the higher clay and silt contents of older soils with desert pavements retain water longer in the upper, most bioavailable portion of the soil profile. This would provide plants more time to transpire the water, perhaps allowing the soil–plant system to be less susceptible to drought. These two characteristics of desert pavements may have profound impacts on ecosystem function in these arid systems. Correspondingly, disruption of these fragile surfaces and the underlying soil structure may have a dramatic

impact on ecosystem function. Further studies will help to elucidate the complex interactions of soil development, hydraulic properties, and ecosystem responses that depend on water entry into soil profiles.

ACKNOWLEDGMENTS

Funding for this research was provided by the Center for Arid Lands Environmental Management of the Desert Research Institute. We acknowledge NSF (EAR 9118335) for support of original soil-geomorphic studies that provided the foundation for this study and the Army Research Office (#DAAD19-00-1-0411) for their support of the initial hydrologic studies. We also thank the anonymous reviewers and Associate Editor for their comments, which improved this manuscript.

REFERENCES

Blake, G.R., and K.H. Hartge. 1986. Bulk density. p. 363–376. *In* A. Klute (ed.) Methods of soil analysis. Part 1. Agron. Monogr. 9. ASA and SSSA, Madison, WI.

Bouma, J., and J.H.M. Wosten. 1979. Flow patterns during extended saturated flow in two, undisturbed swelling clay soils with different macrostructures. Soil Sci. Soc. Am. J. 43:16–22.

Briones, O., C. Montana, and E. Ezcurra. 1998. Competition intensity as functions of resource availability in a semiarid ecosystem. Oecologia 116:365–372.

Brown, K.J., and D.L. Dunkerley. 1996. The influence of hillslope gradient, regolith texture, stone size and stone position on the presence of a vesicular layer and related aspects of hillslope hydrologic processes: A case study from the Australian arid zone. Catena 26:71–84.

Bull, W.B. 1991. Geomorphic responses to climatic change. Oxford Univ. Press. New York.

Casey, F.X.M., and N.E. Derby. 2002. Improved design for automated tension infiltrometer. Soil Sci. Soc. Am. J. 66:64–67.

Cooke, R.U., A. Warren, and A. Goudie. 1993. Desert geomorphology. UCL Press, London.

Eagleson, P.S. 2002. Ecohydrology: Darwinian expression of vegetation form and function. Cambridge Univ. Press, New York.

Gardner, W.R. 1958. Some steady-state solutions of the unsaturated moisture flow equation with application to evaporation from a water table. Soil Sci. 85:228–232.

Hammerlynck, E.P., J.R. McAuliffe, E.V. McDonald, and S.D. Smith. 2002. Impacts of desert soil processes and drought on contrasting Mojave Desert shrubs. Ecology 83:768–779.

Jarvis, N.J., and I. Messing. 1995. Near-saturated hydraulic conductivity in soils of contrasting texture measured by tension infiltrometers. Soil Sci. Soc. Am. J. 59:27–34.

Lide, D.R. 2001. Handbook of chemistry and physics. 82nd ed. CRC Press, Boca Raton, FL.

Lin, H.S., K.J. McInnes, L.P. Wilding, and C.T. Hallmark. 1998. Macroporosity and initial moisture effects on infiltration rates in Vertisols and vertic intergrades. Soil Sci. 163:2–8.

Lin, H.S., K.J. McInnes, L.P. Wilding, and C.T. Hallmark. 1999. Effects of soil morphology on hydraulic properties: I. Quantification of soil morphology. Soil Sci. Soc. Am. J. 63:948–954.

Logsdon, S.D., and D.B. Jaynes. 1993. Methodology for determining hydraulic conductivity with tension infiltrometers. Soil Sci. Soc. Am. J. 57:1426–1431.

McDonald, E.V. 1994. The relative influences of climatic change, desert dust, and lithologic control on soil-geomorphic processes and hydrology of calcic soils formed on Quaternary alluvial-fan deposits in the Mojave Desert, California. Ph.D. diss. Univ. New Mexico, Albuquerque.

McDonald, E.V. 2002. Numerical simulations of soil water balance in support of revegetation of damaged military lands in arid regions. Arid Land Res. Manage. 16:277–290.

McDonald, E.V., L.D. McFadden, and S.G. Wells. 2003. Regional response of alluvial fans to the Pleistocene-Holocene climatic transition, Mojave Desert, California. p. 189–206. *In* N. Lancaster et al. (ed.) Paleoenvironments and paleohydrology of the Mojave and Southern Great Basin Deserts. GSA Spec. Pap. 368. GSA, Boulder, CO.

McDonald, E.V., F.B. Pierson, G.N. Flerchinger, and L.D. McFadden. 1996. Application of a process-based soil-water balance model to evaluate the influence of Late Quaternary climate change on soil-water movement in calcic soils. Geoderma 74:167–192.

McFadden, L.D., E.V. McDonald, S.G. Wells, K. Anderson, J. Quade, and S.L. Forman. 1998. The vesicular layer of desert soils: Genesis and relationship to climate change and desert pavements based on numerical modeling, carbonate translocation behavior, and stable isotope and optical dating studies. Geomorphology 24:101–145.

McFadden, L.D., S.G. Wells, and M.J. Jercinovich. 1987. Influences of eolian and pedogenic processes on the origin and evolution of desert pavements. Geology 15:504–508.

Mohanty, B.P., and Z. Mousli. 2000. Saturated hydraulic conductivity and soil water retention properties across a soil-slope transition. Water Resour. Res. 36:3311–3324.

Mualem, Y. 1976. A new model for predicting the hydraulic conductivity of unsaturated porous media. Water Resour. Res. 12:513–522.

Phillips, F.M. 1994. Environmental tracers for water movement in desert soils in the American southwest. Soil Sci. Soc. Am. J. 58: 15–24.

Porporato, A., P. D'Odorico, F. Laio, L. Ridolfi, and I. Rodriguez-Iturbe. 2002. Ecohydrology of water-controlled ecosystems. Adv. Water Resour. 25:1335–1348.

Shafer, D.S., M.H. Young, S.F. Zitzer, E.V. McDonald, and T.C. Caldwell. 2004. Coupled environmental processes and long-term performance of landfill covers in the Mojave Desert. DRI Publ. 45203. DRI, Las Vegas, NV.

Šimunek, J., R. Angulo-Jaramillo, M. Schaap, J.-P. Vandervaere, and M.Th. van Genuchten. 1998. Using an inverse method to estimate the hydraulic properties of crusted soils from tension disc infiltrometer data. Geoderma 86(1–2):61–81.

Šimunek, J., M. Šejna, and M.Th. van Genuchten. 1999. HYDRUS-2D/MESHGEN-2D software for simulating water flow and solute transport in two-dimensional variably saturated media. Version 2.0. IGWMC-TPS-53C. International Ground Water Modeling Center, Colorado School of Mines, Golden, CO.

Soil Survey Staff. 1998. Soil survey manual. USDA Handb. 18, 8th ed. Soil Conservation Service, U.S. Gov. Print. Office, Washington, DC.

van Genuchten, M.Th. 1980. A closed-form equation for predicting the hydraulic conductivity of unsaturated soils. Soil Sci. Soc. Am. J. 44:892–898.

Watson, K.W., and R.J. Luxmoore. 1986. Estimating macroporosity in a forest watershed by use of a tension infiltrometer. Soil Sci. Soc. Am. J. 50:578–582.

White, I., and M.J. Sully. 1992. On the variability and use of the hydraulic conductivity alpha parameter in stochastic treatments of unsaturated flow. Water Resour. Res. 28:209–213.

Wooding, R.A. 1968. Steady infiltration from a shallow circular pond. Water Resour. Res. 4:1259–1273.